Sirte University Scientific Journal Vol. 16, No. 1 (2026) 205-213
Sirte University Scientific Journal (SUSJ)
Journal home page: http://journal.su.edu.ly/index.php/susj

Calibrating the GHP_{PS} Model Using Cation Exchange Capacity for Improved Resistivity Interpretation in Heterogeneous Sandstones

Fathi Ali Swaid

Civil Department, Faculty of Engineering, Sirte University, Sirte, Libya.

Corresponding author E-mail: *fathi.swaid@su.edu.ly*

DOI: https://doi.org/10.37375/susj.v16i1.4181

ARTICLE INFO:

Received 5 May 2026.
Accepted 18 June 2026.
Available online 24 June 2026.

Keywords: (cation exchange capacity (CEC); GHP_{PS} model; Archie's Law; Vadose Zone)

A B S T R A C T

Estimating water saturation in the vadose zone is a complex challenge in hydrological applications. Traditional models like Archie's Law often fail in clay-bearing formations due to neglecting surface conduction and assuming a fixed saturation exponent. This study calibrates the Glover-Hole-Pous (GHP) model and its partially saturated extension (*n*) using data from Wildmoor Formation sandstone cores. Under full saturation, the geometry factor (*m*) ranged from 1.62 to 1.86, and surface conductivity varied between 10.23 and 24.0 mS/m. Under partial saturation, the (*n)* ranged from 0.49 to 0.77, significantly lower than Archie's canonical value. Analysis revealed strong correlations between *n*, cation exchange capacity (*CEC*), and volumetric charge density (*Qv*), confirming that clay content controls surface conductivity and dictates the saturation-conductivity relationship. These results provide a reliable framework for determining field-scale pore water salinity and saturation. The synergy between model parameters and *CEC* allows constraining GHP and GHP_{PS} models using field measurements, enhancing the interpretation of electromagnetic induction and resistivity surveys. This approach significantly improves the predictability of pore water salinity variations, overcoming traditional limitations. It offers a precise tool for managing water resources and assessing environmental risks in complex clay-bearing formations. By integrating laboratory parameters with field geophysical data, the study establishes a rigorous methodology for improved subsurface characterization, ensuring accurate hydrological modeling and effective environmental monitoring in heterogeneous environments where conventional methods often yield unreliable results for practical applications and decision-making processes in water resource management.

معايرة نموذج (GHP_{PS}) باستخدام السعة التبادلية الكاتيونية لتطوير تفسير المقاومة الكهربائية في الصخور الرملية غير المتجانسة

فتحى على صويد

القسم المدنى،كلية الهندسة ، جامعة سرت، سرت، ليبيا

الـمُخلص

يُعدّ التقدير الدقيق لتشبع الماء في النطاق غير المشبع أحد أهم التحديات وأكثرها تعقيدًا في التطبيقات الهيدرولوجية والبيئية. ومع ذلك، غالبًا ما تفشل النماذج التقليدية، مثل قانون (Archie's Law)، في التكوينات الحاملة للطين, بسبب إهمالها التوصيل السطحي وافتراضها معامل تشبع ثابت($n = 2$). يكز هذا البحث على معايرة نموذج غلوفر–هول–بوس (GHP) وامتداده المشبع جزئيًا (GHP_{PS})باستخدام بيانات تجريبية عالية الجودة من عينات لبية من الحجر الرملي الترياسي لتكوين وايلدمور (Taylor & Barker, 2002, 2006). في ظل ظروف التشبع الكامل، تراوح عامل الهندسة (m) بين 1.62 و1.86، وتراوحت الموصلية السطحية (σr) بين 10.23 و24.0 ملي سيمنز/متر. علاوة على ذلك، في حالة التشبع الجزئي، تراوح معامل التشبع (n) بين 0.49 و0.77، مما يُظهر انخفاضًا ملحوظًا مقارنةً بالقيمة المتعارف عليها لأرتشي. والأهم من ذلك، أظهر n ارتباطات خطية قوية مع سعة التبادل الكاتيوني(CEC) ، ($R^2 = 0.91$وكثافة الشحنة الحجمية Qv) ، .($R^2 = 0.895$وبالمثل، ارتبطت σr ارتباطًا وثيقًا بسعة التبادل الكاتيوني (CEC) .(R^2=0.70) تؤكد هذه النتائج أن محتوى الطين لا يتحكم فقط في الموصلية السطحية، بل يُحدد أيضًا السلوك الوظيفي للعلاقة بين التشبع والموصلية. أظهرت النتائج التي تم الحصول عليها باستخدام نموذج GHP_{PS} أن معامل التشبع (n) للعينات التجريبية يتراوح بين 0.49 و0.77. تُظهر هذه القيم ارتباطات قوية مع السعة التبادلية الكاتيونية (R^2=0.91) ومعدل التدفق الحجمي بالإضافة إلى ذلك، يُسهم التفاعل القوي بين n و m و σr مع السعة التبادلية الكاتيونية في تقييد نموذجي GHPو GHP_{PS} باستخدام قياسات السعة التبادلية الكاتيونية الميدانية. ويُعزز استخدام هذه النماذج المقيدة لتفسير مسوحات التصوير بالحث الكهرومغناطيسي والمقاومة الكهربائية من إمكانية التنبؤ بملوحة المياه المسامية. كما يسمح بتقييد نموذجي GHP و GHP_{PS}عن طريق قياس السعة التبادلية الكاتيونية في الحقل. ويُعزز استخدام هذه النماذج المقيدة لتفسير مسوحات التصوير بالحث الكهرومغناطيسي والمقاومة الكهربائية من إمكانية التنبؤ بتغيرات ملوحة المياه المسامية.

الكلمات المفتاحية: السعة التبادلية للكاتيونات (***CEC***), نموذج GHP_{PS}, قانون أرشي, نطاق عدم التشبع

1 Introduction

The electrical conductivity of unsaturated geological materials is a fundamental property in hydrogeophysics, with critical implications for groundwater monitoring, modeling of contaminant transport, and unsaturated zone characterization (Glover, 2022; Xia et al., 2026).
Conventional empirical approaches, such as (Archie, 1942), apply Archie's Law, by assuming geological media as (clean, clay-free porous media). By linking electrical conductivity solely to porosity, stable fluid conductivity, and water saturation, these models neglect clay-induced surface conduction. This limitation introduces significant errors in petrophysical interpretations, particularly within fine-grained, partially saturated geological formations (Worthington & Pallatt, 1990).
In clayey sediments, electrical conduction is not restricted to the pore fluid; it extends to the mineral-fluid interfaces via the Electric Double Layer (EDL), a phenomenon known as surface conduction (Revil & Glover, 1997; Xia et al., 2026). This dual-conduction mechanism (combining bulk and surface conduction) governs the relationship between saturation and conductivity. thus, using fixed values for the cementation factor (m) or the saturation exponent (n), as done in conventional models, proves inaccurate for estimating water content in real-world hydrogeological environments (Takakura, 2009).
To address these shortcomings, generalized approaches were developed as a framework, such as Glover-Hole-Pous (GHP) framework. The GHP model explicitly integrates geometric (corrugated) and electrochemical (surface conductivity) parameters, enabling more accurate predictions across different saturation states, (Swaid, 2009). Similarly, recent modifications, such as the GHP model for partially saturated media (GHP_{PS}), have enhanced this approach by linking the saturation exponent (n) to the physical and chemical properties of the geological medium, specifically the cation exchange capacity (*CEC*) and the volumetric charge density (Qv), quantities that accurately reflect the clay mineral content and reactivity, (Prakoso et al., 2025).
Cation exchange capacity (*CEC*) is defined as the total amount of exchangeable cations per unit mass of soil, serving as a key indicator of surface conduction potential. While previous studies have linked *CEC* closely to electrical behavior in unsaturated media (Revil & Niu, 2022), experimental validation) GHP) based models remains limited. This is particularly true for heterogeneous natural sandstones under partial saturation conditions (Fu et al., 2021; Demarco et al., 2007). Here, The study focus on studying this gap by applying the GHP and GHPPS approaches using high-quality experimental data from Triassic sandstone samples of the Wildmore Formation (Taylor and Parker, 2002, 2006).
This study aims to: (i) evaluate the variation in the values of the geometric factor (m) and surface conductivity (σs) under full saturation conditions; (ii) determine the extent to which the saturation exponent (n) depends on the cation exchange capacity (*CEC*) and charge density (Qv) at partial saturation; and (iii) verify the possibility of employing the cation exchange capacity (*CEC*) as a direct field parameter for constraining and improving electrical models in the vadose zone. of the results. Sample text inserted for illustration.

2 Materials and Methods

2.1. Data Source
This study is based on an analysis of the experimental database derived from Taylor and Barker (2002, 2006), which includes detailed laboratory measurements performed on core samples of Triassic sandstone from the Wildmore Formation (UK). The measured data cover the rock's total electrical conductivity (σb) and pore water conductivity (σw) under fully saturated (17 samples) and partially saturated (15 samples) conditions. The database also includes, for each sample, values for porosity (ϕ), cation exchange capacity (CEC, in meq/100), and bulk charge density (Qv); these are essential geochemical indices that reflect the clay content and its surface reactivity.

2.2. Theoretical Framework
The theoretical analysis in this study is based on the Glover-Hall-Boss (GHP) model developed by Glover et al. (2000), which represents a generalized extension of Archie's law, the model incorporates two parallel conduction pathways: volumetric (total) conduction through the porous solution, and surface conduction arising at the metal-liquid interaction interfaces. Under full saturation, the model is expressed by the equation (1):

$$\sigma_b = \sigma_w \phi^m + \sigma_r (1-\phi)^P \dots\dots\dots\dots (1)$$

Where:

- σb is bulk electrical conductivity (S/m),
- σw is pore water conductivity (S/m),
- ϕ is porosity,
- m is the geometric (cementation) factor,
- σr is surface (grain) conductivity (S/m),
- $P = \log(1-\phi^m)/(\log(1-\phi)$, is a grain geometry exponent (Glover et al., 2000).

To address partial saturation, the model is extended following Swaid (2009), who introduced the GHP Partial Saturation (GHPPS) model by incorporating the saturation exponent (n) via Archie's resistivity index concept. The resulting expression is (equation 2):

$$\sigma_{PS} = S_w^n \left(\sigma_r (1-\phi)^{\left(\frac{\log(1-\phi^m)}{\log(1-\phi)}\right)} + \sigma_r \phi^m \right) \dots\dots\dots.. (2)$$

Where Sw is water saturation. In this formulation, n is no longer a fixed empirical constant but a variable dependent on geochemical properties such as *CEC* and Qv.

2.3. Two-Stage Calibration Procedure
The calibration process was performed in two consecutive stages using the nonlinear least Squares Levenber g- Marquardt algorithm, implemented via Gnuplot™ (Press et al., 2007).
Stage 1: Calibration under full saturation conditions.
Equation (1) was matched with the bulk conductivity (σb) versus pore water conductivity (σw) data from the

17 fully saturated cores to estimate the values for each core of both of the geometric factor (m) and surface conductivity (σr). The importance of this step lies in isolating the effect of pore geometry and surface conductivity arising from the clay components at full saturation ($Sw = 1$).

Stage 2: Calibration of partial saturation conditions

Based on the n and σr values calibrated in Stage 1, Equation (2) was used to data from 15 partially saturated core samples to estimate the saturation exponent (n), considering the degree of saturation (Sw) and pore water conductivity (σw) as known inputs. This step ensures the complete isolation of the saturation exponent (n) from geometric and surface influences, allowing for an independent and accurate assessment of its dependence on clay properties.

2.4. Correlation and Validation Analysis

To assess the dependence of electrical parameters on geochemical properties, linear regression analyses were performed between:

- n and *CEC* (cation exchange capacity),
- n and Qv (clay charge per unit volume),
- σr (rock electrical conductivity) and *CEC*.

The model's performance was also evaluated by comparing the parameters derived from the GHP model with those derived from the Hanai - Bruggeman (H-B) effective medium theory (Hanai, 1960; Bruggeman, 1935), which represents a physically accurate alternative for modeling heterogeneous media.

3 Results

3.1. Outputs of fully saturated calibration

17 Triassic sandstone core samples in the fully saturated state were used to calibrate the GHP model. Accordingly, the geometric coefficient (m) values were recorded in the range of 1.62 –1.86, and the surface conductivity (σr) values in the range of 10.24–24.0 mS/m, as shown in Table 1. . The model calibration of (σ_b) versus (σ_w) for fully saturated cores data are shown in Figure 2. Statistics confirm the accuracy of these outputs, with relative standard errors of less than 1.6% and 5.7% for the geometric coefficient and surface conductivity, respectively.

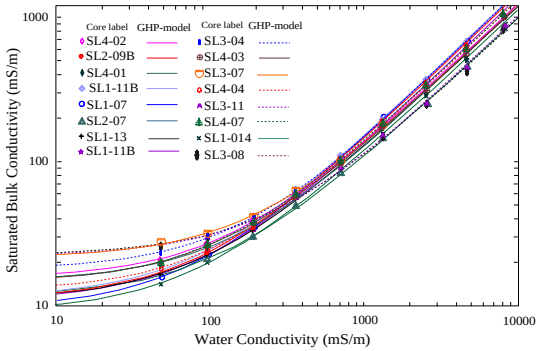

Figure 1: GHP model calibration of bulk conductivity (σ_b) versus pore water conductivity (σ_w) for fully saturated cores

Table 1: Petrophysical, Geochemical, and GHP-Derived Electrical Parameters of Fully Saturated Sandstone Cores

Core ID	ϕ	m	σ_r *mS/m*	Q_v *meq/ml*	CEC meq/100g
SL1-07	0.28	1.63	10.833	0.06	0.84
S11-B11	0.29	1.62	13.055	0.18	2.67
S11-13	0.28	1.66	12.412	0.11	1.54
SL1-14	0.26	1.64	10.248	-	-
S12-07	0.26	1.73	13.065	-	-
S12-A9	0.27	1.65	12.33	0.18	2.54
S12-9B	0.28	1.65	12.30	0.18	2.54
S13-04	0.27	1.69	19.30	0.4	5.61
S13-07	0.26	1.67	23.17	0.33	4.21
S13-08	0.26	1.86	24.0	0.51	6.74
S13-09	0.26	1.85	23.86	0.41	5.45
S13-11	0.25	1.79	23.72	0.33	4.13
S14-01	0.29	1.86	16.33	-	-
S14-02	0.29	1.72	17.806	0.19	2.97
S14-03	0.29	1.71	16.37	0.22	3.47
S14-04	0.29	1.74	14.20	0.23	3.47
S14-07	0.29	1.72	16.35	0.15	2.31

(-) Data not available

A weak correlation was observed between m and porosity (ϕ), with a coefficient of determination of R^2=0.05. In contrast, moderate to strong linear relationships were found between m and cation exchange capacity (*CEC*) (R^2 = 0.56), and between σr and *CEC* (R^2 = 0.70).

3.2. Partial Saturation Calibration

Application of the GHP_{PS} model to 15 partially saturated cores produced saturation exponent (n) values ranging from 0.49 to 0.77 (Table 2). The model fits to bulk conductivity versus water saturation data are shown in Figure 2.

Table 2: Geochemical Properties and Electrical Parameters of Partially Saturated Sandstone.

Core ID	ϕ	m	σ_r *mS/m*	Q_v *meq/ml*	CEC *eq/100g*	n
SL1-07	0.28	1.63	10.8	0.06	0.84	0.49
S11-B11	0.28	1.62	13.1	0.18	2.67	0.55
S11-13	0.28	1.66	12.4	0.11	1.54	0.51
SL1-14	0.26	1.64	10.3	-	-	0.53
S12-07	0.26	1.73	13.1	-	-	0.59
S12-A9	0.27	1.65	12.3	0.18	2.54	0.54
S12-9B	0.28	1.65	12.3	0.18	2.54	0.54
S13-04	0.27	1.69	19.3	0.4	5.61	0.77
S13-07	0.26	1.67	23.2	0.33	4.21	0.68
S13-11	0.25	1.79	23.7	0.33	4.13	0.62
S14-01	0.29	1.86	16.3	-	-	0.54
S14-02	0.29	1.72	17.8	0.19	2.97	0.58
S14-03	0.29	1.71	16.4	0.22	3.47	0.61
S14-04	0.29	1.74	14.2	0.23	3.47	0.59
S14-07	0.29	1.72	16.4	0.15	2.31	0.51

(-) Data not available

Strong linear correlations were identified between n and *CEC* (R^2 = 0.91), (Figure 3) and between n and

volumetric charge density (Qv) (R^2 = 0.896) (Figure 4). The corresponding regression equations are:

$$n = 0.0602\,CEC + 0.4003 \ldots\ldots\ldots (3)$$
$$n = 0.7782Qv + 0.4165 \ldots\ldots\ldots\ldots (4)$$

Where *CEC* is in meq/100 g and *Qv* in meq/ml.

Additionally, a moderate linear relationship was observed between σr and n (R^2 = 0.48) (Figure 5).

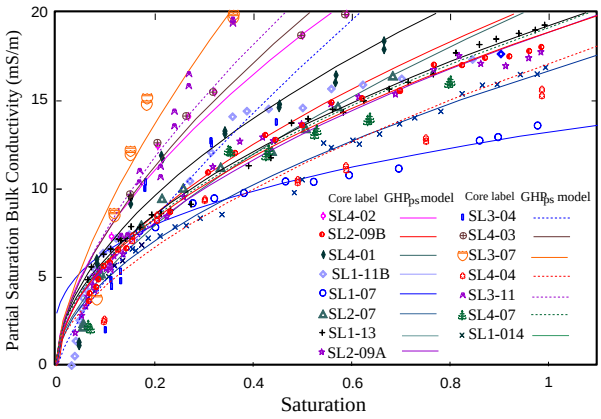

Figure 2: GHP_{PS} Model Fit: Bulk Conductivity (σb) versus Water Saturation (Sw) for Partially Saturated Cores

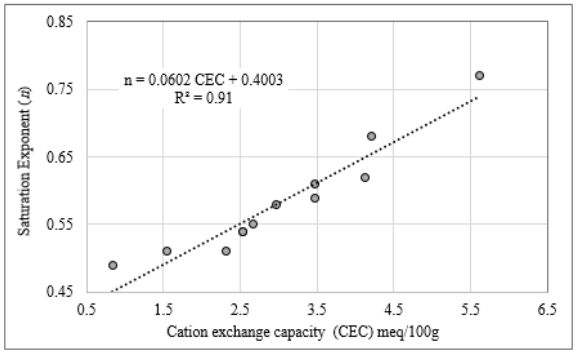

Figure 3: Linear Correlation between Saturation Exponent (n) and Cation Exchange Capacity (CEC) (R^2=0.91)

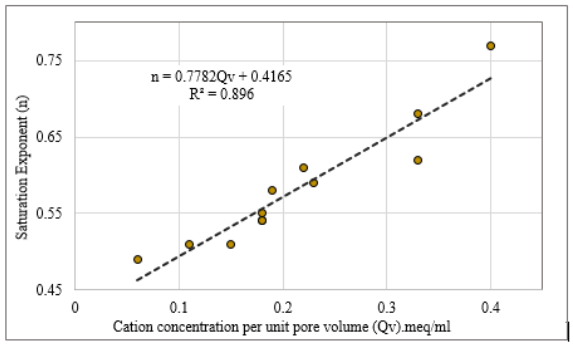

Figure 4: Linear Correlation between Saturation Exponent (n) and Volumetric Charge Density (Qv), showing Regression (R^2 = 0.896).

3.3. Model Comparison: GHP vs. Hanai–Bruggeman (H–B)

Comparison of GHP-derived parameters with those obtained from the Hanai–Bruggeman (H–B) effective medium theory (Taylor & Barker, 2006) showed strong agreement. The correlation coefficients were R^2 = 0.896 for m and R^2 = 0.48 for σr (Figures 4 and 5). On average, GHP underestimated σr by 13.8%, while the deviation in m was negligible (0.78% lower). A sample-wise summary is provided in Table 3.

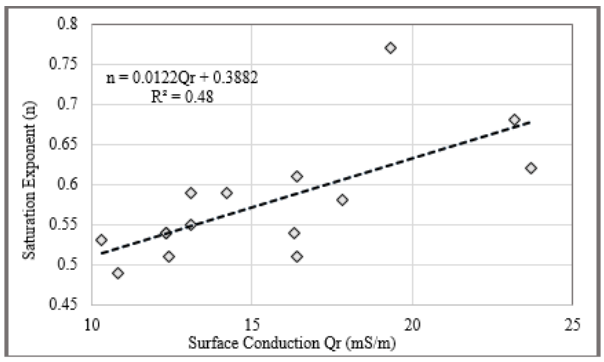

Figure 5: Surface Conduction (σr) versus Saturation Exponent (n), Showing the Linear Regression Relationship (R^2 = 0.48).

3.4. Estimation of n from Soil Texture

Using Equation (3) and typical *CEC* ranges from Donahue et al. (1977), a lookup table was developed to estimate n from soil texture (Table 4). For example:

- Sandy soils (*CEC* = 1–5 meq/100 g) correspond to $n \approx 0.46 – 0.70$,
- Clay loams (*CEC* = 15 – 30 meq/100 g) yield $n \approx 1.31 – 2.22$.

This relationship is visualized in Figure 6.

Table 3. Estimated ranges of the saturation exponent (n) based on soil texture and corresponding cation exchange capacity (CEC) values (Donahue et al., 1977).

Soil texture	Donahue et al., 1977 data	Predicted data
	CEC (meq/100g, of soil)	Estimating (n) value corresponding to Figure (4)
Sand	1 – 5	0.46 - 0.70
Fine sandy loams	5 – 10	0.70 – 1.01
Loams and silt loams	5 – 15	0.70 – 1.31
Clay loams	15 – 30	1.31 – 2.22
Clay	30 +	2.22 +

4. Discussion

4.1. Revisiting the Saturation Exponent: Beyond Archie's Assumption

Contrary to the traditional assumption of Archie's model, (1942), which posits a constant saturation exponent (n) of 2 in cohesive sandstone formations, our current results reveal a lower value for this coefficient in Triassic sandstone, ranging from 0.49 to 0.77. This radical variation undermines the accuracy of classical

calculations when applied to clay-rich and unsaturated zones. These findings support the recent research trend (Zhang et al., 2023) that rejects the notion of absolute constancy for the coefficient n, emphasizing its dynamic nature related to the spatial structure of pores and electrochemical interactions.

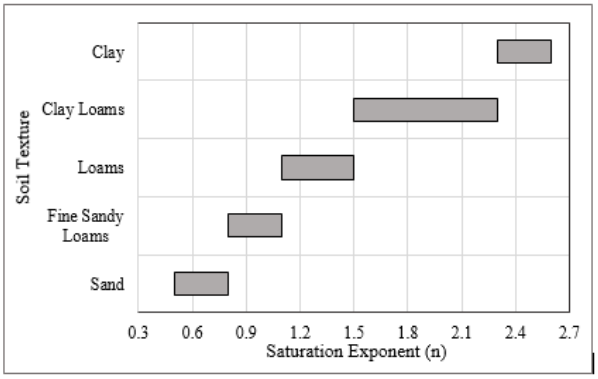

Figure 6: Estimated ranges of the saturation exponent (*n*) based on soil texture

The increasing clay content in the rock leads to a radical shift in the nature of the relationship between conductivity and saturation. This phenomenon is attributed to the simultaneous increase in both the corrugation and specific surface area of the clay minerals, which positively impacts surface conductivity and limits the expected drop in overall conductivity at low water saturation (Revil et al., 2020; Lesmes & Frye, 2021). This physical mechanism explains why high saturation exponent (*n*) values are associated with samples that have high cation exchange capacity, a behavior that is completely contrary to the simplified Archie model. These conclusions gain high reliability due to the strong linear correlations observed between n and both cation exchange capacity (*CEC*, $R^2 = 0.91$) and volumetric charge density (*Qv*, $R^2 = 0.896$)

4.2. Dependence of *CEC* in Electrical Modeling of Complex Media

The current study presents cation exchange capacity (*CEC*) as an effective field diagnostic tool for refining electrical modeling and interpreting heterogeneity in complex geological environments. The competitive advantage of *CEC* compared to traditional physical properties such as porosity or grain size distribution lies in its comprehensive ability to integrate electrochemical activity, surface reactivity, and rock mineral composition into a single, independent variable. Furthermore, this indicator gains practical applicability due to its ability to be routinely obtained through standard soil testing (Donahue et al., 1977). The practical value of the equations derived in our study is embodied in:

$$n = 0.0606 \,.\, CEC + 0.3986$$

$$n = 0.783 \,.\, Qv + 0.4149$$

in its ability to provide a realistic alternative, grounded in precise geochemical indicators, to address the shortcomings of the default standard value (*n* =2). This formulation falls within the emerging research framework dedicated to upscaling geophysical data, where the joint constraint of geochemical and geophysical data serves as an essential tool to reduce inversion ambiguity and interpretation uncertainty (Weller et al., 2022; Slater et al., 2021). This alignment extends to field applications; a study by Ishihara & Tsukamoto (2004) demonstrated that formulating models based on the Generalized Reciprocal Method (*CEC*) ensures more reliable outputs for water content and salinity in electromagnetic induction measurements, thereby providing a robust physical justification for our calibration process

4.3. Model Validation: GHP vs. Effective Medium Theory

The adoption of the GHP model as a practical and physically robust alternative in field applications is attributed to its exceptional agreement with the theoretically rigorous H-G effective medium theory, yielding a coefficient of determination of $R^2 = 0.889$ for the parameter m and R2 = 0.959 for the conductivity σr. Furthermore, the GHP formulation achieves a comparable accuracy to H-G models without requiring their complex microstructural assumptions; the GHP model is constrained by only two fitting parameters (m , σr), making it an ideal choice for data scarce environments (Taylor & Barker, 2006). Although there is a slight underestimation of 13.8% in the σr values predicted by GHP which is likely linked to the simplistic reduction of pore geometry, particularly in clay-rich samples where the electrical double layer overlaps (Revil & Glover, 1997) this marginal deviation remains highly acceptable. This tradeoff is justified by the computational efficiency and high physical interpretability the model provides, both of which are critical advantages for real time monitoring of the vadose zone.

4.4. Implications for Hydrogeophysical Practice

The current findings of this study open up significant application prospects for characterizing the vadose zone using electrical resistivity methods. The most prominent implications are as follows:

- Overcoming systematic errors: Replacing the fixed Archie exponent with values of n governed by cation exchange capacity (CEC) is a necessary step to avoid systematic errors when calculating salinity and saturation levels.
- Improving the quality of field surveys: Electromagnetic induction (EMI) and electrical resistivity tomography (ERT) surveys can be based on the proposed data table (Table 4) to produce more accurate maps and distributions of groundwater moisture.
- Enhancing the efficiency of pollution models: Geophysical-based pollutant transport simulation models will benefit from the improved input accuracy, thus reducing the uncertainty associated with estimates of pore water salinity and saturation (Binley et al., 2021).

Accordingly, this study contributes to bridging the existing gap between soil chemistry, rock physics, and geophysical hydrology by linking measurable geochemical properties to electrical response

coefficients; this supports the adoption of more integrated strategies in the fields of environmental monitoring and natural resource management

4.5. Limitations and Future Directions

Despite the promising results of this study, its scope remains limited to Triassic sandstone formations. Further validation is needed, including different rock environments such as carbonate rocks, volcanic ash (tuff), and anthropogenic soils, to assess the generalizability of these models. Furthermore, investigating the effect of pore fluid chemistry (e.g., pH, salinity, and ion type) on the n-CEC relationship is an important avenue of research, given the role of ionic strength in modifying bilayer thickness and surface conductivity mechanisms (Yoon et al., 2002; Revil et al., 2020). In this context, future research should incorporate spectroscopic induction polarization (SIP) as an independent tool for constraining Qv and CEC values (Wang et al., 2021), offering a robust pathway toward fully coupled petrophysical-geochemical inversions. This methodological advancement serves as the missing link to bridge the current observational gap, harmonizing discrete, high-precision laboratory measurements with continuous hydro-geophysical imaging at the field scale

5. Conclusions and Recommendations

5.1. Conclusions

This study provides experimental proof of the efficiency of the geometry model (GHP) and its partially saturated extension (GHP_{PS}) following their successful calibration using high-quality core samples from the Triassic sandstone of the Wildmore Formation (Taylor & Barker, 2002, 2006).

Measurements under full saturation conditions revealed a geometric coefficient (m) ranging from 1.62 to 1.86 and a surface conductivity (σr) ranging from 10.23 to 24.0 mS/m. while, under partial saturation, the saturation exponent (n) showed a significant decrease, ranging from 0.49 to 0.77, deviating from the traditional Archie value (n =2). The results gain physical depth due to the close linear correlations observed between n and both the cation exchange capacity (*CEC*, R2 = 0.91) and the volumetric charge density (Qv, R^2 = 0.895), as well as the strong coupling between σr and *CEC* (R^2 = 0.70). This demonstrates that the clay components reshape the functional regime linking saturation and electrical conductivity in unsaturated bands, in addition to controlling surface conductivity.

Furthermore, the physical reliability of the GHP model is reinforced by its exceptional conformity with the rigorous analytical formulation of the Hanay - Brugmann (H-B) effective medium theory, achieving correlation coefficients of R^2 = 0.889 for m and R^2 = 0.959 for σr. This makes it a superior and mechanically accurate tool for field hydrogeophysical applications

5.2 Recommendations

The practical value of this work lies in formulating proposals for the scientific and engineering communities concerned with geophysical hydrology and soil ecology, as follows:

1. Adopting *CEC* as a field constraint: Integrating cation exchange capacity analyses into geoelectrical survey protocols for unsaturated zones ensures increased reliability of saturation and salinity models based on electromagnetic induction and resistivity data (Yoon et al., 2002; Kwader, 1985).
2. Moving towards a dynamic saturation exponent: It is recommended to abandon reliance on the standard Archie value (n = 2) in clay media and use variable values related to the electrochemical response of *CEC*, by activating the following empirical equations:

$$n = 0.0606.\,CEC + 0.3986, (CEC\ in \frac{meq}{100g})$$

$$n = 0783.\,Qv + 04149\ (Q_v\ in\ \frac{meq}{ml})$$

3. Integrating Geophysical and Geochemical Data: Geochemical and geophysical indicators should be integrated into hydrological models. The co-correlation of *CEC*, Qv, and electrical conductivity enhances the predictive power of models used to assess slope stability, irrigation system efficiency, and pollutant transport (Weller et al., 2022; Binley et al., 2021).
4. Expanding the Validation of the GHP_{PS} Model: It is essential to test the validity of the GHPPS model across diverse lithological environments including carbonate rocks, volcanic deposits, and anthropogenic soils to assess its generalizability beyond Triassic sandstones.
5. Employing Spectroscopic Induced Polarization (SIP) Techniques: It is recommended to incorporate SIP measurements into subsequent studies to provide independent determinants of both *Qv* and *CEC* (Slater et al., 2021), thus paving the way for the development of fully coupled petrophysical-geochemical inversion models.
6. Developing Intelligent Field Protocols: It is recommended to develop field mechanisms that combine rapid *CEC* estimation (using handheld sensors or inferential indicators) with real-time electrical resistivity imaging, enabling high-resolution, adaptive monitoring of the unsaturated band in agricultural and environmental settings.

5.3 For broader methodological perspectives:

This work contributes to the development of hydrogeophysics literature by establishing mathematical frameworks that link electrical responses to geochemical variables. This provides researchers with a flexible model for relating field geophysical measurements to the chemical properties of soil structure under the influence of electrochemical processes. The role of the developed GHP_{PS} model, constrained by *CEC* values, is highlighted as an integrative tool capable of standardizing research metrics by transferring laboratory petrophysical calibrations to comprehensive field geophysical imaging applications. This methodological shift constitutes a fundamental pillar for overcoming the arbitrariness of

traditional interpretations and achieving graphical analysis based on coherent physical foundations and highly reliable electrical data.

References

Archie, E., (1942) the electrical resistivity log as an aid in determining some reservoir characteristics. Transactions of the AIME, 146(1), 54–62. https://doi.org/10.2118/942054-G

Binley, A., Slater, L., & Revil, A., (2021) Advances in the application of electrical resistivity models for vadose zone characterization. Journal of Hydrology, 595, Article 125974. https://doi.org/10.1016/j.jhydrol.2021.125974

Bruggeman, G. (1935) Berechnung verschiedener physikalischer Konstanten von heterogenen Substanzen. Annalen der Physik, 416(8), 636–664. https://doi.org/10.1002/andp.19354160802

Demarco, M., Jahns, E., Rüdrich, J., Oyhantcabal, P., & Siegesmund, S. (2007) the impact of partial water saturation on rock strength: An experimental study on sandstone. Zeitschrift Der Deutschen Gesellschaft Für Geowissenschaften, 158(4), 869–882. https://doi.org/10.1127/1860-1804/2007/0158-0869

Donahue, L., Hester, E., & Smith, R. (1977) Surface conduction and its relationship to saturation exponents in porous media. Geophysics, 42(1), 112–124. https://doi.org/10.1190/1.1440712

Fu, Q., Zhang, Z., Zhao, X., Hong, M., Guo, B., Yuan, Q., & Niu, D. (2021) Water saturation effect on the dynamic mechanical behaviour and scaling law effect on the dynamic strength of coral aggregate concrete. Cement and Concrete Composites, 120, 104034. https://doi.org/10.1016/j.cemconcomp.2021.104034

Glover, J., (2022). Electrical properties of partially saturated rocks: A review of recent advances. Geophysical Journal International, 228(3), 1820–1845. https://doi.org/10.1093/gji/ggab410

Glover, J., Hole, J., & Pous, J. (2000) A modified Archie's law for two conducting phases. Earth and Planetary Science Letters, 180(3–4), 369–383. https://doi.org/10.1016/S0012-821X (00)00168-5

Hanai, T., (1960) Theory of the dispersion of dielectric constant and dielectric loss of emulsions and suspensions. Kolloid-Zeitschrift, 171(1), 23–31. https://doi.org/10.1007/BF01513154

Ishihara, K. and Tsukamoto, Y., (2004) cyclic strength of imperfectly saturated sands and analysis of liquefaction. Proc Jpn Acad Ser B Phys Biol Sci. 80 (8):372 – 91. PMCID: PMC8153656.

Kwader, T. (1985) Influence of cation exchange capacity on electrical conductivity in clay-rich sediments. Clays and Clay Minerals, 33(5), 435–442. https://doi.org/10.1346/CCMN.1985.0330508

Lesmes, P., & Frye, M., (2021) the role of surface conduction in controlling electrical properties of fine-grained sediments. Water Resources Research, 57(4), Article e2020WR028934. https://doi.org/10.1029/2020WR028934

Prakoso, S., Burhannudinnur, M., Herdiansyah, F., Rahmawan, S., & Prakoso, B. A. (2025) Assessing pore quality impact on saturation exponent and water saturation calculation. Journal of Petroleum Exploration and Production Technology, 15(8), 129. https://doi.org/10.1007/s13202-025-02028

Press, W. H., Teukolsky, S. A., Vetterling, W. T., & Flannery, B. P. (2007). Numerical recipes: The art of scientific computing (3rd ed.). Cambridge University Press.

Revil, A. & Glover, J., (1997) Theory of ionic surface electrical conduction in porous media. Physical Review B, 55(3), 1757–1773. https://doi.org/10.1103/PhysRevB.55.1757

Revil, A., Jougnot, D. & Leroy, P. (2020) Modeling the electrical conductivity of sedimentary rocks: A review. Earth-Science Reviews, 204, Article 103178. https://doi.org/10.1016/j.earscirev.2020.103178

Revil, A., Vaudelet, P., Su, Z. & Chen, R., (2022) Induced Polarization as a Tool to Assess Mineral Deposits: A Review. Minerals, 12(5), 571. https://doi.org/10.3390/min12050571

Slater, L., Ntarlagiannis, D. & Weller, A., (2021) Advances in spectral induced polarization for hydrogeological applications. Surveys in Geophysics, 42(5), 1075–1109. https://doi.org/10.1007/s10712-021-09663-7

Swaid, F., (2009) Estimating a new approach for describing electrical conductivity parameters in partially saturated sediments. WIT Transactions on Ecology and the Environment, 127, 361–370. https://doi.org/10.2495/RAV090321

Takakura, S., (2009) Influence of pore-water salinity and temperature on resistivity of clay-bearing rocks. BUTSURI-TANSA (Geophysical Exploration), 62(4), 385–396. https://doi.org/10.3124/segj.62.385

Taylor, K. & Barker, J., (2002) Petrophysical properties of Triassic sandstones from the Wildmoor Formation. Geological Society, London, Special Publications, 200(1), 45–60. https://doi.org/10.1144/GSL.SP.2002.200.01.04

Taylor, K. & Barker, J., (2006) further studies on the electrical properties of Triassic sandstone samples. Journal of Applied Geophysics, 59(3), 245–258. https://doi.org/10.1016/j.jappgeo.2005.09.001

Wang, C., Briggs, A., Day-Lewis, D. & Slater, L., D. (2021) Characterizing Physical Properties of Streambed Interface Sediments Using In Situ Complex Electrical Conductivity Measurements. Water Resources Research, 57(2), e2020WR027995. https://doi.org/10.1029/2020WR027995

Weller, A., Slater, L., Binley, A. & Ntarlagiannis, D., (2022) Applications of electrical resistivity imaging in hydrogeological and environmental investigations. Surveys in Geophysics, 43(2), 345–370. https://doi.org/10.1007/s10712-021-09673-5

Worthington, F. & Pallatt, N., (1990) Effect of Variable Saturation Exponent upon the Evaluation of Hydrocarbon Saturation. SPE Annual Technical Conference and Exhibition, SPE-20538-MS. https://doi.org/10.2118/20538-MS

Xia, T., Li, M., Slater, L., Hu, X., Binley, A., Ma, X. & Mao, D., (2026) the Evolving Roles of Electrical Geophysical Methods for In Situ Remediation Assessment: Progress and Perspectives. Water Resources Research, 62(4), e2025WR043172. https://doi.org/10.1029/2025WR043172

Yoon, S., Yee, N. & Werkema, D., (2002) Effects of pore water salinity and cation exchange capacity on electrical conductivity of porous media. Environmental Science & Technology, 36(15), 3375–3381. https://doi.org/10.1021/es015701t

Zhang, X., Liu, H. & Wang, Y., (2023) Advances in geophysical modeling of vadose zone processes using electrical conductivity data. Advances in Water Resources, 171, Article 104356. https://doi.org/10.1016/j.advwatres.2022.104356